

## **Elucidating the degradation mechanism of the cathode catalyst of PEFC by a combination of electrochemical methods and X-ray fluorescence spectroscopy**

J. Monzó<sup>1</sup>, D. van der Vliet, A. Yanson<sup>2</sup> and P. Rodriguez<sup>1</sup>

<sup>1</sup> University of Birmingham. School of Chemistry, Birmingham. B15 2TT, UK.

<sup>2</sup> Cosine Measurement Systems, Oosteinde 36, 2361 HE Leiden. The Netherlands

Corresponding author: [p.b.rodriguez@bham.ac.uk](mailto:p.b.rodriguez@bham.ac.uk)

### **Table of contents**

Section 1. Microscopic confirmation of homogeneous catalyst layer.

Section 2. Experimental design to determine Pt content within the catalyst layer.

Section 3. Calibration curve and limit of detection for Pt content.

Section 4. Calibration curve and limit of detection for TaC content.

Section 5. Particle size distribution of Pt-Nps.

Section 6. Compositional analysis of Pt/TaC by XRF.

Section 7. Physical characterization of Pt/Vulcan catalyst.

Section 8. ORR Tafel plots of the catalysts: Pt-Nps, Pt/Vulcan and Pt/TaC.

Section 9. Study of the mechanical stability of the Nafion-free catalyst layer.

Section 10. Fluorescence spectra of the catalyst layer as a function of number of cycles during the load cycle protocol.

Section 11. Average of the particle size of each catalyst as a function of number of cycles during the load cycle protocol and shut-up/shut-down protocol.

Section 12. ORR Tafel plots as a function of number of cycles during the load cycle protocol.

Section 13. Fluorescence spectra of the catalyst layer as a function of number of cycles during the start-up/shut-down protocol.

Section 14. Fluorescence spectra of Pt/TaC ( $\text{Ta}_{L\alpha}$ ) layer as a function of number of cycles during the start-up/shut-down protocol.

Section 15. ORR Tafel plots of catalysts as a function of number of cycles during the start-up/shut-down protocol.

**Section 1. Microscopic confirmation of homogeneous catalyst layer.**

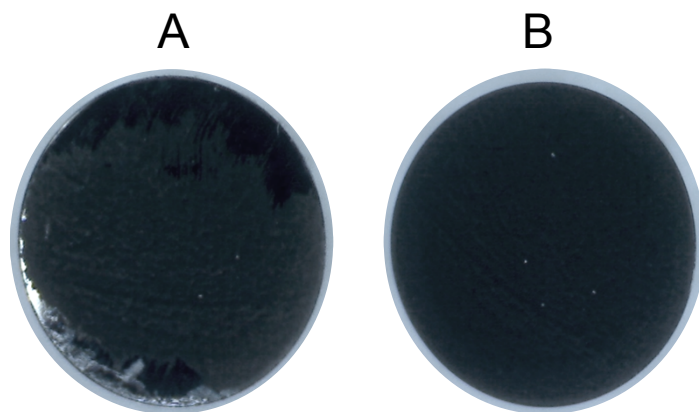


**Figure S11.** Optical micrograph of the film obtained using (A) the one-drop casting method and (B) the film obtained using the multi-drop casting method proposed in this work.

## **Section 2. Experimental design to determine Pt content within the catalyst layer.**

In order to establish a relationship between the electrochemical surface area (ECSA) and Pt content, to distinguish between associative and dissociative processes, the Pt content of the catalyst layer on the disk was determined by X-ray fluorescence (XRF). After a well-defined number of degradation cycles, the working electrode was placed in a XRF spectrometer and the Pt content was resolved. To reduce the background noise, the best scan quality provided by the equipment was employed for all the measurement carried out in this work. These measurements took 25 minutes each under helium atmosphere.

After the Pt content characterization, the carbon disk was polished with 0.05  $\mu\text{m}$  alumina to remove all the catalyst from the carbon disk surface. After the polishing, the carbon disk was sonicated for 10 minutes and dried in an air-flow oven at 55 °C. In order to confirm the absence of any remaining catalyst on the carbon surface, the disk was characterized by XRF prior to its next use. Then, a new thin catalyst layer was prepared to proceed with the degradation protocols.

### Section 3. Calibration curve and limit of detection for Pt content.

In order to establish a relationship between the XRF response and the Pt content, an experimental calibration curve was constructed. A certain volume of Pt solution with a well-known concentration of Pt ( $125 \mu\text{g mL}^{-1}$ ) was deposited on a zero response carbon disk and allowed to evaporate in air. The dried carbon disk was then analysed by XRF with each Pt loading on the disk investigated in triplicate (table S11).

*Table S11. Experimental data for Pt calibration curve.*

Mass Pt $\pm 0.1$ ( $\mu\text{g}$ )	Net intensity $\pm 1$ (Cps)		
8.0	1464	1515	1634
6.9	1408	1427	1339
5.9	1195	1253	1199
4.8	951	868	960
3.7	729	762	799
2.6	618	515	614
1.5	315	335	355
0.7	234	167	177
1.2	275	290	230
2.2	399	490	465

Figure S12 shows the calibration plot using the net intensity of Pt<sub>L $\alpha$</sub>  signal (9.45 KeV) as a function of the mass of Pt deposited on the carbon disk. As can be seen, the response of the intensity is linearly proportional to the mass of Pt with a correlation coefficient of 0.996.

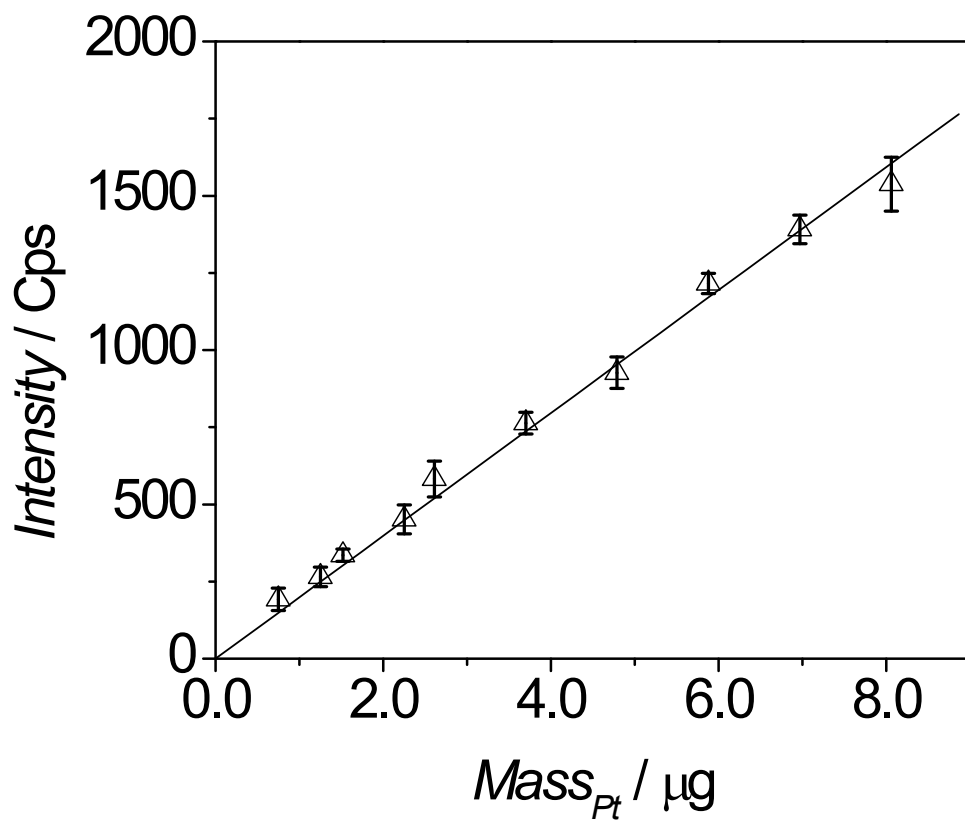


**Figure SI2.** Calibration data for Pt detection by XRF spectrometer (gradient =  $199 \pm 3$  Cps  $\mu\text{g}^{-1}$ ,  $R^2 = 0.998$ ).

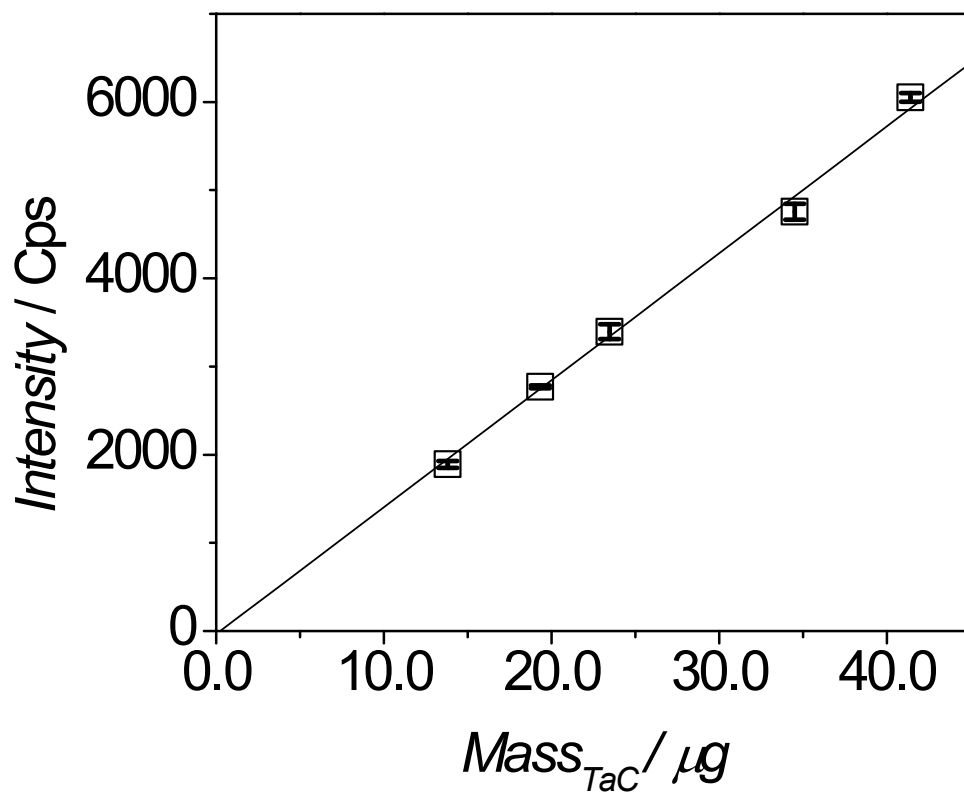
#### Section 4. Calibration curve and limit of detection for TaC content.

In order to establish a relationship between the XRF response and the TaC content, an experimental calibration curve was constructed. The protocol followed was the same used for the calibration curve of detection of Pt, section 3.

*Table SI2. Experimental data for TaC calibration curve.*

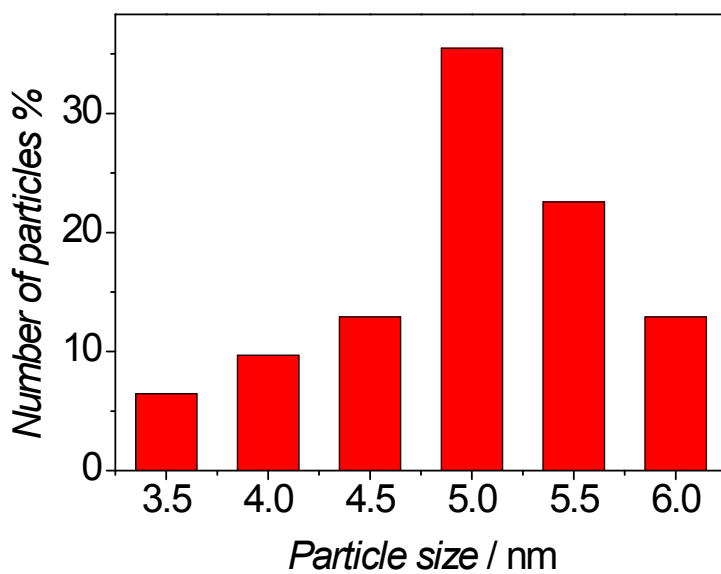
<b>Mass <math>p_t \pm 0.1</math> (<math>\mu\text{g}</math>)</b>	<b>Net intensity <math>\pm 1</math> (Cps)</b>		
23.5	1464	1515	1634
19.3	1408	1427	1339
34.5	1195	1253	1199
41.4	951	868	960

Figure SI3 shows the calibration plot using the net intensity of TaC<sub>L $\alpha$</sub>  signal (8.45 KeV) as a function of the mass of TaC deposited on the carbon disk.



**Figure S13.** Calibration data for TaC detection by XRF spectrometer (gradient =  $144 \pm 4$  Cps  $\mu g^{-1}$ ,  $R^2 = 0.999$ ).

## Section 5. Particle size distribution of Pt-Nps.



**Figure S14.** Particle size distribution of Pt-Nps obtained from TEM measurements. The relative abundance of each particle size was calculated from a total of 175 nanoparticles.

## Section 6. Compositional analysis of Pt/TaC by XRF.

A layer of Pt/TaC was deposited on the surface of a zero background response carbon disk. Then, this carbon disk was placed in a XRF spectrometer, acquiring the composition of this prepared catalyst. The compositional analysis was done in triplicate, resulting in a composition of  $(19.6 \pm 0.8) \% \text{ Pt}$  and  $(80.4 \pm 0.8) \% \text{ Ta}$ .

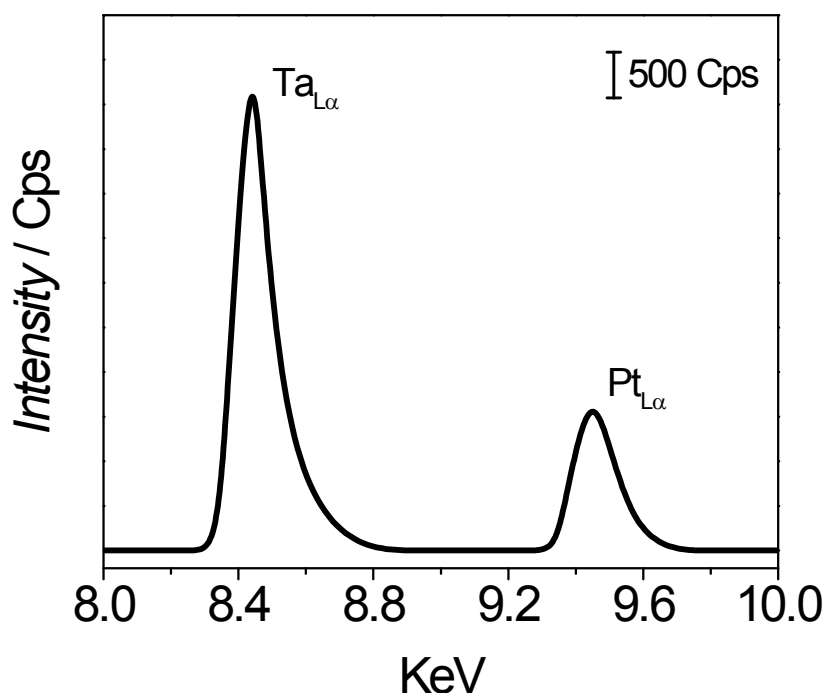


**Figure SI5.** X-ray fluorescence spectra of Pt nanoparticles supported on TaC. The signals at 8.45 keV and 9.45 keV are associated to Ta<sub>Lα</sub> and Pt<sub>Lα</sub> respectively. In order to present clear results, the original data was digitalized using the *GraphClick* software. Original data is available upon request.

## Section 7. Physical characterization of Pt/Vulcan catalyst.

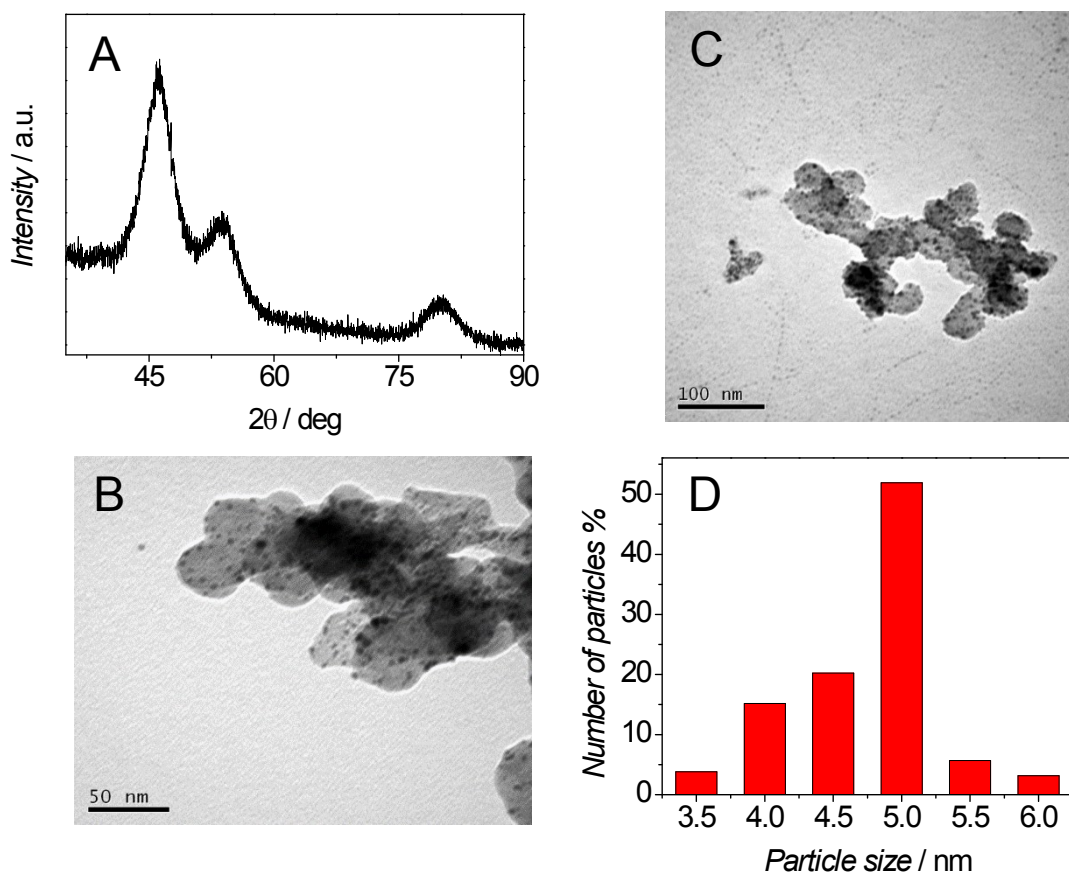


**Figure S16.** (A) XRD pattern, (B-C) TEM images and (D) particle size distribution of Pt/Vulcan catalyst. The relative abundance of each particle size was calculated from a total of 175 nanoparticles.

Section 8. ORR Tafel plots of the catalysts: Pt-Nps, Pt/Vulcan and Pt/TaC.

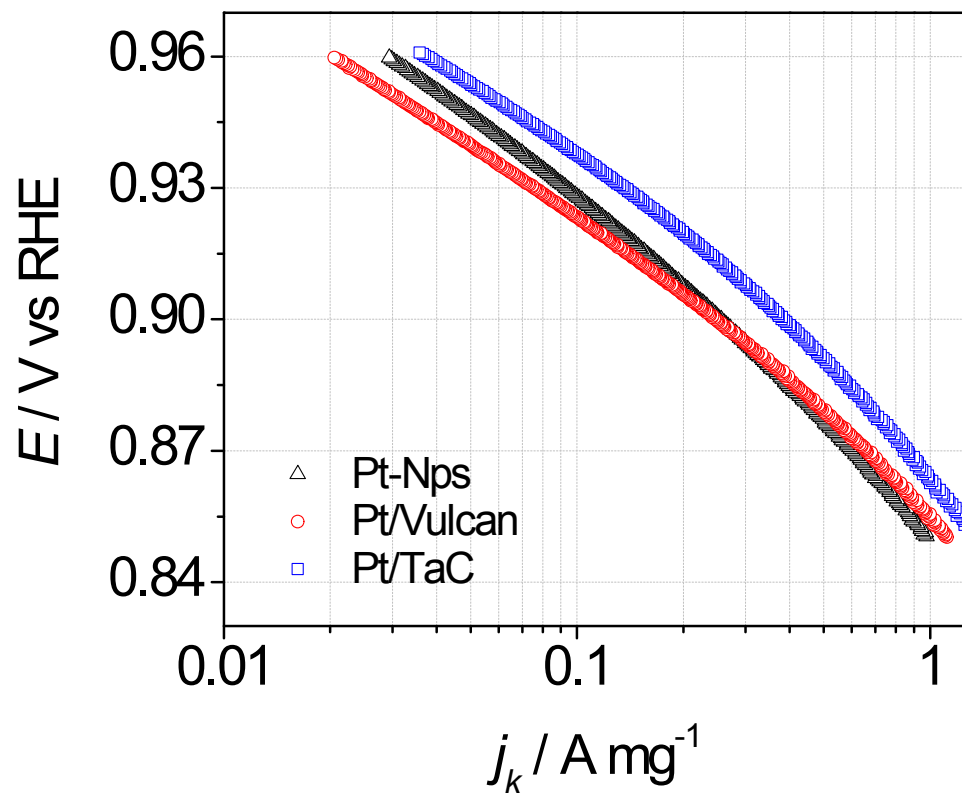


**Figure S17.** Mass activity,  $j_k$ , for the ORR on Pt-Nps, Pt/Vulcan and Pt/TaC, data are shown for the positive-going sweep at  $20 \text{ mVs}^{-1}$  in  $\text{O}_2$ -saturated  $0.1 \text{ M HClO}_4$  at 1600 rpm.

## Section 9. Study of the mechanical stability of the Nafion-free catalyst layer.

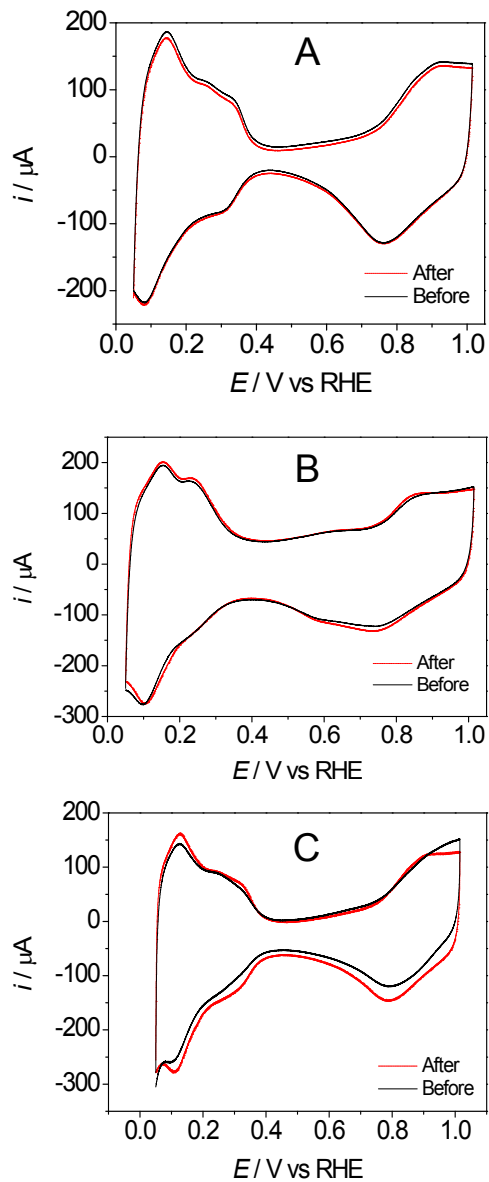


**Figure S18.** Voltammetric profiles of Pt-nps (A), Pt/Vulcan (B) and Pt/TaC (C) before (black line) and after (red dashed line) mechanical stress evaluation. The catalysts were rotated at 300 rpm in 0.1 M  $\text{HClO}_4$  during 5 hours at open circuit potential. The voltammograms were carried out in 0.1 M  $\text{HClO}_4$  at  $50 \text{ mVs}^{-1}$ .

**Section 10. Fluorescence spectra of the catalyst layer as a function of number of cycles during the load cycle protocol.**

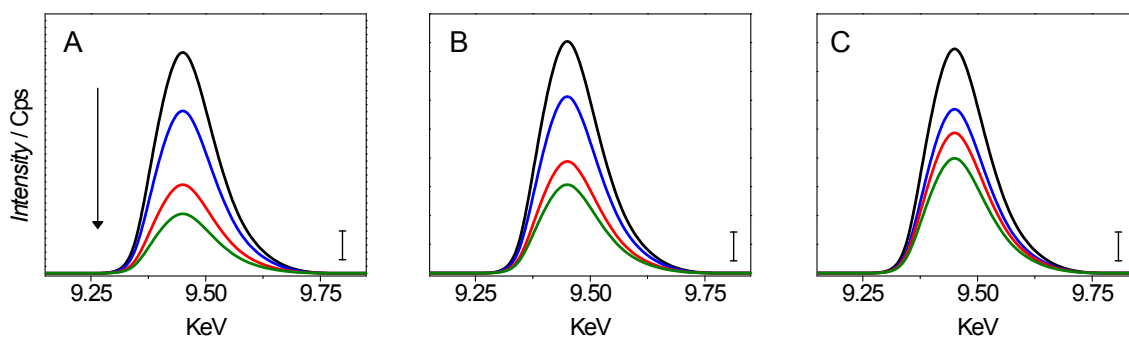


**Figure S19.** X-ray fluorescence spectra ( $Pt_{L\alpha}$ ) of Pt-Nps (A), Pt/Vulcan (B) and Pt/TaC (C) at different stages of the load cycle protocol; 0 cycles (black line), 2000 (blue line), 6000 cycles (red line) and 10000 cycles (green line). The scale bar corresponds to 100 Cps intensity. In order to present clear results, the original data was digitalized using the *GraphClick* software. Original data is available on request.

**Section 11. Average of the particle size of each catalyst as a function of number of cycles during the load cycle protocol and shut-up/shut-down protocol.**

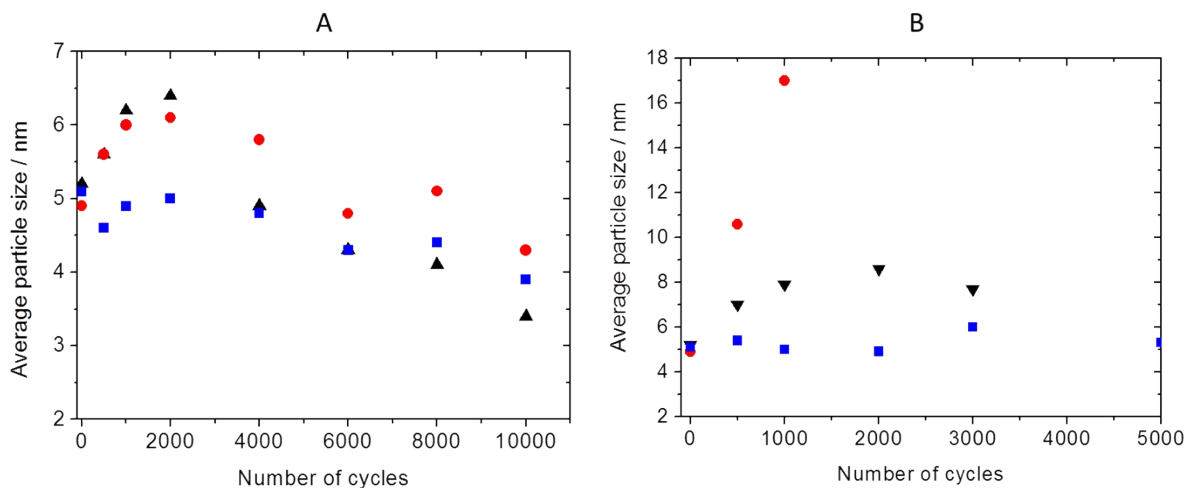


**Figure SI 10. Average particle size of the Pt nanoparticles calculated from the mass of platinum and the ECSA as a function of the number of cycles for (A) load cycle protocol and (B) start-up/shut-down protocol. Pt-Nps (black), Pt/TaC (blue) and Pt/Vulcan (red).**

**Section 12. ORR Tafel plots as a function of number of cycles during the load cycle protocol.**

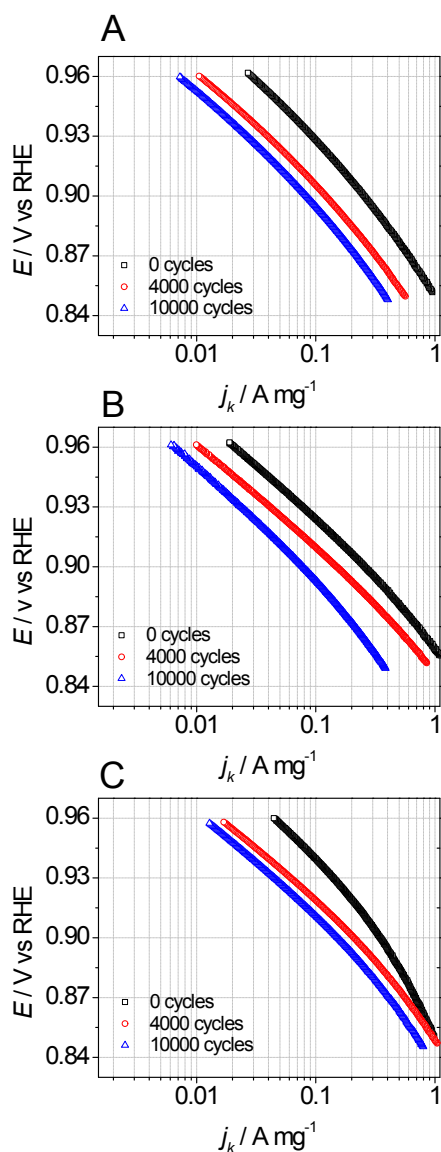


**Figure S11.** Mass activity,  $j_k$ , for the ORR on Pt-Nps (A), Pt/Vulcan (B) and Pt/TaC (C) as a function of number of degradation cycles during the load cycle protocol. Data are shown for the positive-going sweep at  $20\text{ mVs}^{-1}$  in  $\text{O}_2$ -saturated  $0.1\text{ M HClO}_4$  at 1600 rpm.

**Section 13. Fluorescence spectra of the catalyst layer as a function of number of cycles during the start-up/shut-down protocol.**

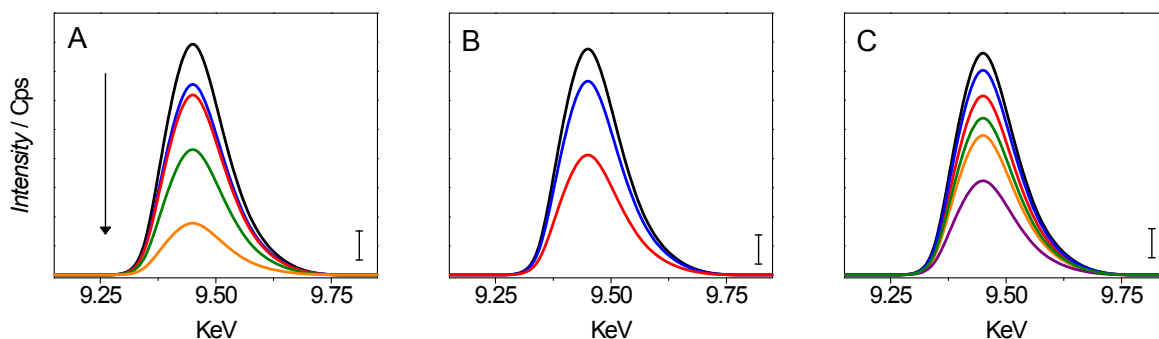


**Figure S112.** X-ray fluorescence spectra of Pt-Nps (A), Pt/Vulcan (B) and Pt/TaC (C) at different stages of the start-up/shut-down protocol. 0 cycles (black line), 500 cycles (blue line), 1000 cycles (red line), 2000 cycles (green line), 3000 cycles (orange line) and 5000 cycles (purple line). The scale bar corresponds to 100 Cps intensity. In order to present clear results, the original data was digitalized using the *GraphClick* software. Original data is available on request.

**Section 14. Fluorescence spectra of Pt/TaC ( $Ta_{L\alpha}$ ) layer as a function of number of cycles during the start-up/shut-down protocol.**

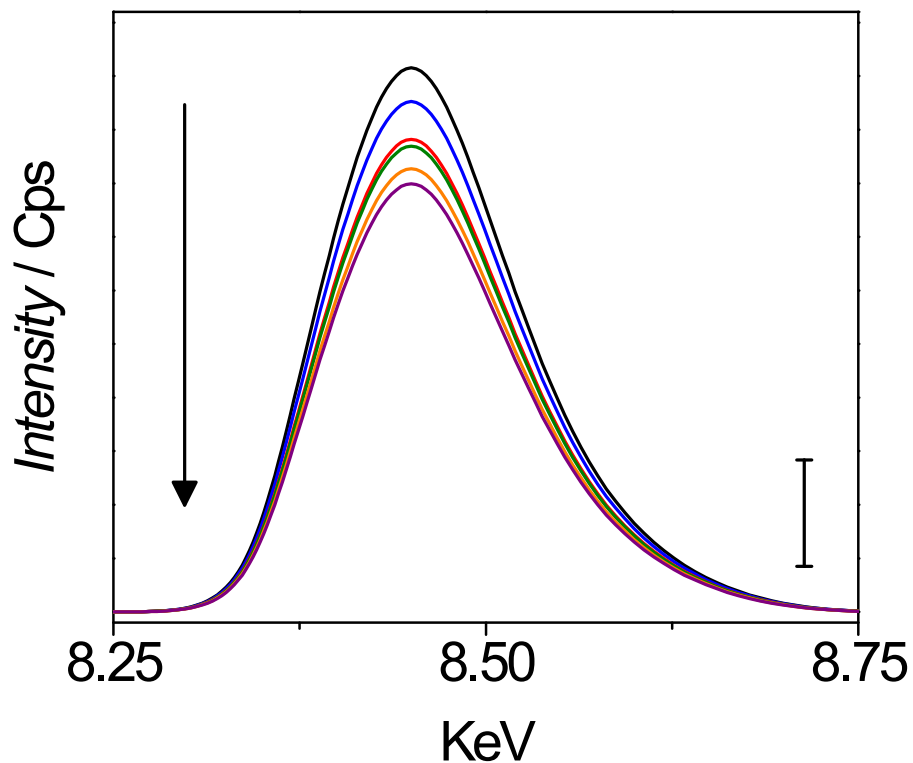


**Figure SI13.** X-ray fluorescence spectrum of Pt/TaC at different stages of the start-up/shut-down protocol. 0 cycles (black line), 500 cycles (blue line), 1000 cycles (red line), 2000 cycles (green line), 3000 cycles (orange line) and 5000 cycles (purple line). The scale bar corresponds to 500 Cps intensity. In order to present clear results, the original data was digitalized using the *GraphClick* software. Original data is available on request.

**Section 15. ORR Tafel plots of catalysts as a function of number of cycles during the start-up/shut-down protocol.**

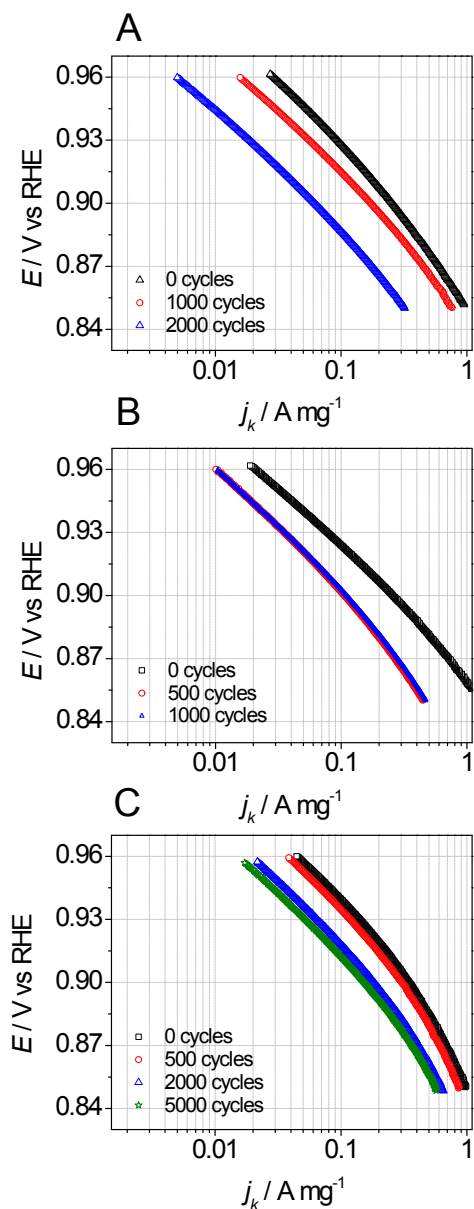


**Figure S114.** Mass activities,  $j_k$ , for the ORR on Pt-Nps (A), Pt/Vulcan (B), and Pt/TaC (C) as a function of number of cycles during the start-up/shut-down protocol. Data are shown for the positive-going sweep at  $20 \text{ mVs}^{-1}$  in  $\text{O}_2$ -saturated  $0.1 \text{ M HClO}_4$  at 1600 rpm.